Colloids and Surfaces A: Physicochem. Eng. Aspects 460 (2014) 460–467

Contents lists available at ScienceDirect

Colloids and Surfaces A: Physicochemical and Engineering Aspects

journal homepage: www.elsevier.com/locate/colsurfa

Structure of flocs of latex particles formed by addition of protein from Moringa seeds☆

Maja S. Hellsing[a], Habauka M. Kwaambwa[b], Fiona M. Nermark[c], Bonang B.M. Nkoane[c], Andrew J. Jackson[d], Matthew J. Wasbrough[e,f], Ida Berts[g], Lionel Porcar[h], Adrian R. Rennie[a,*]

[a] Materials Physics, Uppsala University, Box 516, SE-75120 Uppsala, Sweden
[b] Polytechnic of Namibia, Natural Sciences Unit, Private Bag 13388, 13 Storch Street, Windhoek, Namibia
[c] Department of Chemistry, University of Botswana, Private Bag UB 00704, Gaborone, Botswana
[d] European Spallation Source ESS AB and Physical Chemistry, Lund University, Box 124, SE-22100 Lund, Sweden
[e] NIST Center for Neutron Research, 100 Bureau Drive, MS 6100, Gaithersburg, MD 20899-6100, USA
[f] Department of Chemical and Biomolecular Engineering, University of Delaware, Newark, DE 19716, USA
[g] Department of Chemistry – Ångström Laboratory, Uppsala University, Box 538, SE-75121 Uppsala, Sweden
[h] Institut Laue Langevin, 6 rue Jules Horowitz, F-38042 Grenoble Cedex 9, France

HIGHLIGHTS

- *Moringa oleifera* seed protein binds strongly to polystyrene latex.
- Seed protein is an effective flocculent creating very dense flocs.
- Fractal dimensions of flocs increase with particle concentration.
- Floc densities are higher than those found with simple ionic coagulants.

GRAPHICAL ABSTRACT

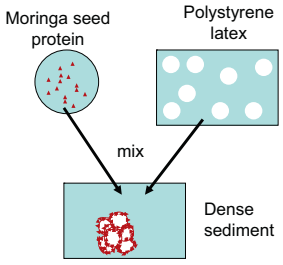

ARTICLE INFO

Article history:
Received 6 October 2013
Received in revised form
20 November 2013
Accepted 21 November 2013
Available online 1 December 2013

Keywords:
Flocculation
Fractal aggregates
Protein adsorption

ABSTRACT

Proteins extracted from the seeds of *Moringa* trees are effective flocculents for particles dispersed in water and are attractive as a natural and sustainable product for use in water purification. Studies with a model system consisting of polystyrene latex particles have shown that the protein adsorbs to the surface and causes flocculation as unusually dense aggregates. Small-angle neutron scattering that exploits contrast matching of deuterated latex particles dispersed in D_2O to highlight bound protein has shown that the adsorbed amount reaches about 3 mg m^{-2}. The particles form very compact flocs that are characterized by fractal dimensions that approach the theoretical maximum of 3. Ultra small-angle neutron scattering allows these flocs to be characterized for a range of particle and protein concentrations. Proteins from two species of *Moringa* trees were investigated. The protein from *Moringa stenopetala* seeds gave rise to slightly lower fractal dimensions compared to *Moringa oleifera*, but still much larger than values observed for conventional ionic or polymeric flocculents that are in the range 1.75–2.3. Compact flocs are desirable for efficient separation of impurities and dewatering of sludge as well as other applications. A trend of increasing fractal dimension with particle concentration was observed when *M. stenopetala* seed protein was used and this resembles the behaviour predicted in Brownian dynamics simulation of flocculation.

* Corresponding author. Tel.: +46 184713596.
E-mail addresses: Maja.Hellsing@physics.uu.se (M.S. Hellsing), Adrian.Rennie@physics.uu.se (A.R. Rennie).

0927-7757/$ – see front matter © 2013 The Authors. Published by Elsevier B.V. All rights reserved.
http://dx.doi.org/10.1016/j.colsurfa.2013.11.038

1. Introduction

The study of flocculation is of wide practical importance as it forms part of many industrial processes, for example in production of ceramics, mineral flotation and the manufacture of coatings. Aggregation of impurities is an important first stage in water purification so that contaminant particles can sediment, cream or be removed easily with filters. The aggregation of particles to form clusters has also been of theoretical interest and many models are based on the early ideas of Smoluchowski [1] about the kinetics of colloidal coagulation. This relates the diffusion of component particles in a fluid to the growth of aggregates. More recently, the idea of self-similar structures [2] on many length scales that are known as fractals has helped in the categorisation of colloidal flocs [3,4]. The probability of finding a particle in an aggregate at a given distance from the centre depends on the density of packing and can be related to an exponent known as the dimension, d, of a mass fractal.

A first stage in most procedures for drinking water treatment and purification is the coagulation and flocculation of particulate impurities [5,6]. The particular motivation for the present work has been to understand the mechanism by which a novel, natural flocculent is effective in water purification. A number of studies have identified that seeds from *Moringa oleifera* trees can be used to clarify water [7,8], and that the active ingredient for this purpose is the seed protein that has an important component with molecular mass of about 6.5 kDa [9]. Recent neutron reflection experiments [10] have identified that the protein binds strongly to silica surfaces and a plateau in the adsorbed amount is reached at solution concentrations as low as 0.3 mg ml^{-1}. Interactions of the protein with surfactants have also been studied. Dynamic light scattering [11] has shown that the protein disperses in water with a hydrodynamic radius of 1.5–2 nm in dilute solution but tends to aggregate when solutions are concentrated. The strong tendency to associate and to bind to a wide variety of interfaces provides an obvious mechanism for the protein to act as a flocculent [10]. Recent reports describe the use of the *M. oleifera* protein in connection with water purification and these include both its role as a coagulant [8,12] and possible antimicrobial action [13]. The requirement to maintain low levels of organic carbon in treated water with added protein has also been addressed specifically [14]. A comparative study has indicated that *M. oleifera* protein is, at present, one of the most effective plant materials that has been tested [15].

The low molecular mass suggests that the protein does not act in the same way as most polymeric flocculents. The present work was initiated to understand the physical processes that are involved in the flocculation of particles by investigating samples in situ using ultra small-angle neutron scattering. The model system of particles chosen for the study was polystyrene latex. Complementary measurements of the adsorption to the surface of these particles are presented. An understanding of the physical processes that govern aggregation under simple quiescent conditions is essential in order to comprehend more complicated behaviour in stirred and flowing dispersions. It should be noted in this respect that the application of protein flocculent has been advocated for use under a very wide range of conditions such as sedimentation in small pots on a domestic scale and in larger treatment plants. The results of the present work are discussed in terms of fractal dimensions that can describe the density of flocs that arise from an aggregation process.

2. Background

2.1. Fractal aggregates

It is convenient to investigate the structure of fractal objects using X-ray, neutron or light scattering as these techniques probe the three-dimensional distribution of density within samples. These experiments are similar in that the intensity, I, is measured as a function of scattering angle, θ, and wavelength, λ. Data is usually reported as a function of the momentum transfer, Q that is given by $Q = (4\pi/\lambda)\sin(\theta/2)$. The mass, m, within a sphere of radius R for a mass fractal is simply given by $m(R) \sim R^d$ and the intensity of scattering is given by [16] $I(Q) \sim Q^{-d}$. There are several well-established models for aggregation that predict specific values of the dimension d. These distinguish whether the property that controls the growth is primarily the diffusion rate or if the probability of a particle sticking to a cluster (reaction) provides the limit. It has been recognized since early experiments of Lin et al. [17–19] that there is likely to be polydispersity in most systems and that small clusters can diffuse and aggregate with other clusters. This has given rise to the terms diffusion limited colloid aggregation (DLCA) and reaction limited colloid aggregation (RLCA). The exponents d for these cases have been identified from experiment, theory and computational models as about 1.85 and 2.1 respectively [17]. RLCA provides a higher density and consequently larger value for the dimensionality, d, than the DLCA process. The higher value of d for RLCA can be understood qualitatively as occurring because particles or small clusters are able to explore more of the free space within an aggregate if the reaction probability rather than diffusion limits the 'sticking'.

Meakin and Jullien [4] have pointed out that mechanisms such as rearrangement within clusters can change the observed dimensionality and give some overlap between the ranges of expected exponents. The paper warns that making only analysis of fractal dimensions of aggregates is inadequate to determine the mechanism and kinetics of their formation. This caveat would apply whether the aggregates are measured using scattering or real-space techniques such as microscopy. However, even if full details of the mechanism that gives rise to a floc may be ambiguous from a structural analysis, the results are important as for example, properties such as mechanical strength [20,21], the sol to gel transition, and the ability to pass through filters [22] will depend on the structure.

There are some further complications to the simple interpretation of scattering from aggregates. A review by Sorensen [23] discusses a number of important points such as the effects of the finite size of the components that form the aggregate, as well as the overall aggregate size that can strongly limit the range in which a power-law scattering behaviour is observed. As the fractal dimension reaches the limiting value of 3 that corresponds to a uniform density in a three-dimensional space, the scattering will necessarily change as there would then be sharp boundaries between clusters. The intensity would then vary as Q^{-4}, as expected in the Porod limit of small-angle scattering. In order to understand the aggregation, it is clearly helpful to measure over a wide range of Q to provide information about the limits at both small and large length scales. The model proposed by Teixeira [24] has been widely used to describe scattering from fractal aggregates of spherical particles.

2.2. Polystyrene latex as model particles

A number of particles have been used as model materials for studies of flocculation. For example, gold particles, silica sols and polystyrene latex have all been demonstrated [17] to fall on the same master curves of scattering data for aggregates if the appropriate conditions as regards stability are chosen for the different dispersions. Most studies that exploit light scattering or microscopy have been restricted to rather dilute samples to avoid strong multiple scattering that would limit investigations to regions very close to walls of containers. The size and concentration of particles have been identified as of considerable interest. Gravitational settling was observed [18,25] and this motion may predominate over diffusion so as to alter the aggregation. Early studies have investigated

polystyrene latex under the influence of a number of different flocculents: Broide and Cohen [26] looked at fast aggregation in the presence of $MgCl_2$. Cationic polymers were used by Gregory [27] who reported that the rate of aggregate formation was independent of molecular mass of polymer but depends on electrolyte concentration. This suggests that under some circumstances addition of polyelectrolytes may act primarily by screening charged repulsion. An antibody–antigen interaction has also been used [28] to provide specific attraction between latex particles. These studies indicate that details of the composition can be used to tune the behaviour.

The simple picture of aggregation behaviour in dilute solutions that emerged from early studies has required extension in a number of ways. The results of Giglio et al. [29–31] showed a clear peak in the scattered intensity in low angle light scattering experiments that was ascribed to flocculation occurring by spinodal decomposition that gives sharp boundaries between separated regions after 'ripening' of the structure. The scaling of the peak position, fractal dimension and time has been related to a diffusion model by Sciortino et al. [32,33].

As a practical model, it is useful to investigate aggregation of particles of a size and at a concentration that is relevant to applications. Computational models have recently suggested that the fractal dimension in a DLCA process decreases with increasing particle size [34]. There have been studies of structures that arise from flocculation that relate particularly to problems in water purification [35]. For example, the settling properties of sludge have been related to the fractal structure of aggregates [36]. The structure of flocs and hence the mechanism of aggregation is of central importance to practical aspects of clarification of contaminated water. Flocs that are densely packed will sediment or float according to the density difference more rapidly than loose aggregates as the viscous drag scales linearly with the hydrodynamic radius.

The results of Brownian dynamics simulations of the effect of concentration have shown a strong variation in fractal dimension with volume fraction [37]. The fractal dimension was observed to increase approximately linearly with volume fraction up to the gel point. Similar results were seen in earlier Monte Carlo simulations in two and three dimensions [38,39].

3. Experimental

3.1. Scattering instruments

The study has used ultra small-angle neutron scattering (USANS) to determine the structure of flocculated polystyrene latex. The technique uses two perfect channel-cut crystals to measure the broadening of a monochromatic neutron beam with wavelength 2.4 Å and thus to measure small-angle scattering from a sample placed between them and access a range of momentum transfer from about 3×10^{-5} to 3×10^{-3} Å^{-1}. The BT5 USANS instrument [40] at the NIST Center for Neutron Research, MD, USA, was equipped with specially constructed mounts that allowed the sample cells to rotate continuously [41] about an axis in the beam direction at approximately 0.2 rad s^{-1} (2 rpm) so as to avoid sedimentation under gravity during the measurements that took about 5–6 h. This range of Q allows the aggregation and floc structure to be investigated with particles that are of sizes relevant to practical problems such as water purification. The samples were contained in 1 mm path length fused quartz cells. Data were reduced using the standard procedures [42] that involved determination of the transmission with respect to an empty cell and normalization as well as subtraction of the background scattering from the empty sample cell. Incoherent scattering from the water, approximately 0.8 cm^{-1}, is an insignificant contribution to the background in the range studied.

Complementary small-angle neutron scattering (SANS) measurements were made to investigate the adsorption of the *M. oleifera* protein to a deuterated polystyrene latex using contrast matching of the particles to highlight the scattering from the adsorbed protein. The data were collected with the 'pinhole' SANS instrument D22 [43] at the Institut Laue Langevin, Grenoble, France using wavelengths of 6 and 12 Å. The two-dimensional position sensitive area detector was placed at two different sample-to-detector distances 5 and 17.6 m to provide a range of Q between 0.0015 and 0.2 Å^{-1}.

The intensity of small-angle scattering depends on the contrast between components in the sample. For neutrons, materials are characterized by a scattering length density, ρ, which depends on the chemical composition and properties of atomic nuclei. For example, normal hydrogen (^{1}H) and deuterium (^{2}H or D) have very different scattering lengths. If a region or component in a sample consists of two components with volume fraction φ_1 and φ_2, then φ_2 is equal to $(1 - \varphi_1)$ and the scattering length density is simply

$$\rho = \varphi_1\rho_1 + \varphi_2\rho_2 = \rho_2 + \varphi_1(\rho_1 - \rho_2).$$

Models that fit ρ can therefore be used to determine the composition in samples. Adjusting the isotopic composition of a solvent allows matching of a particular component so that other species can be identified. These ideas are used in the experiments described below to investigate adsorption of protein to latex particles.

The Bonse–Hart geometry for the USANS camera provides good collimation in one direction defined by the Bragg diffraction from the channel-cut crystals but the beam is smeared in the perpendicular direction. The most convenient analysis is usually to convolute appropriate models of scattering with the instrument resolution in a computer program and this was the procedure followed in the present study rather than desmearing the experimental data [44].

3.2. Materials

The polystyrene latices used in these experiments were synthesized in Uppsala. The hydrogenous latex chosen for the flocculation experiments is designated PS3 and was prepared following the procedure of Goodwin et al. [45]. A smaller, deuterated latex (PSD1) was used for studies of protein adsorption. Details of the syntheses are provided in the supporting information.

Moringa stenopetala seeds were purchased in Ethiopia. *M. oleifera* seeds were obtained from a farmer in Gaborone, Botswana. The *Moringa* proteins were purified at the University of Botswana as described previously by Maikokera and Kwaambwa [46,47] following the method of Ndabigengesere and Narasiah [48]. The densities and scattering length densities for the various materials used are listed in Table 1. Protein solutions were prepared by mass from the freeze-dried powder.

Table 1
Properties of materials.

Material	Formula	Density (g cm^{-3})	Scattering length density, $\rho/10^{-6}$ Å^{-2}
Water	H_2O	0.997	−0.56
Heavy water	D_2O	1.105	6.35
Polystyrene	C_8H_8	1.055	1.41
Deuterated polystyrene	C_8D_8	1.14	6.44
Moringa oleifera protein		1.36	2.89[a]
Moringa stenopetala protein		1.4[b]	2.9

[a] Value for protein that has exchanged in D_2O.
[b] Assumed to be similar to *Moringa oleifera* protein.

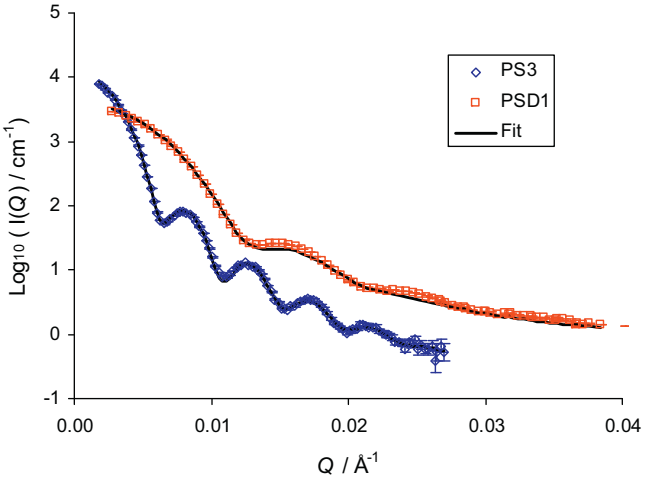

Fig. 1. Scattering from dilute dispersions of the polystyrene latices (about 0.5 % by mass) used for the experiments with protein with added NaCl (1×10^{-3} mol l^{-1}). These measurements of the form factor for the hydrogenous latex PS3 in D_2O (blue diamonds) and deuterated particles PSD1 (red squares) in H_2O show the mean radii to be 721 ± 5 and 362 ± 15 Å respectively. (For interpretation of the references to color in this text, the reader is referred to the web version of the article.)

3.3. Characterization of particles and proteins

The small angle scattering data for the polystyrene latices dispersed in water with 1×10^{-3} mol l^{-1} NaCl are shown in Fig. 1. Uncertainties are indicated as one standard deviation in the text and as bars in all figures. The radii from the model fits are listed in Table 2. These parameters were used in the subsequent analysis of data for particles with adsorbed protein and the flocculated latex. Fuller description of the characterization of the deuterated latex in different water contrasts [49] with mixtures of H_2O and D_2O and of the hydrogenous latex including the effects of multiple scattering [52] are provided elsewhere. The zeta potentials for both latices were about −35 mV.

The amino acid analyses of both purified protein products are reported in the Supporting Information. There are only small differences in the overall amino acid composition of the two proteins that are similar to those between different batches of *M. oleifera* protein. Light scattering studies reported previously [11] indicate that dilute solutions of the *M. oleifera* protein contain species with hydrodynamic radius of 15–20 Å. At high concentrations such as 2 mg ml^{-1} the solutions of proteins are cloudy; light scattering and turbidity measurements indicate that large aggregates are formed. At pH 7 the zeta potential for *M. oleifera* in solution at a concentration 0.5 mg ml^{-1} is +20 mV [11].

The preparation procedure (mixing sequence) for the samples in this study was always to add the protein from a stock solution with concentration 4 mg ml^{-1} to the dispersion of particles. For the cases where additional pure water was added, the addition sequence was first latex, followed by water and finally protein. One exception was the sample containing mass fractions 0.02 of the PS3 latex and 2 mg ml^{-1} *M. oleifera* protein, for which the pure water was added as the last ingredient. All latex was taken from the original stock with volume fraction of 0.087, except for one sample where the latex fraction was 0.005 (*M. oleifera* 2 mg ml^{-1}). This sample was prepared from a diluted stock with mass fraction 0.012 latex. For the samples containing additional salt, the NaCl was added as the last ingredient, from a 0.01 mol l^{-1} stock solution.

Table 2
Radii of polystyrene latex particles used.

Material	Designation	Radius (Å)
Hydrogenous latex	PS3	721 ± 5
Deuterated latex	PSD1	362 ± 15

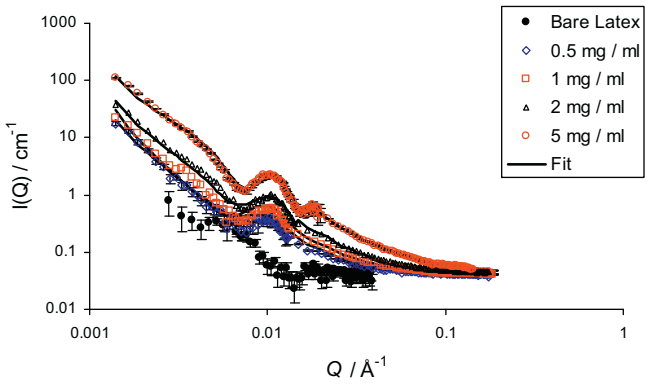

Fig. 2. Small-angle scattering from the deuterated latex in D_2O with added *Moringa oleifera* protein. The samples with different protein concentrations are shown with fits to a core–shell model with residual protein that accounts for the adsorbed layer. More details of the protein scattering are provided in the supporting information.

4. Results and discussion

4.1. Adsorption of protein to latex

The scattering for the deuterated latex PSD1 in D_2O with 1×10^{-3} mol l^{-1} NaCl is shown in Fig. 2 along with that for samples with added *M. oleifera* protein. For measurements in D_2O, the scattering length density of the deuterated polystyrene latex particles almost matches the solvent and the observed signal arises predominantly from the adsorbed layer. As a consequence, the scattering for the particles without any added protein is very weak. The large difference due to the protein is clear and the shape of the curve resembles that for core-shell structures with a high contrast for the shell. The upturn at small Q is indicative of some aggregation. There could be contributions to this scattering from aggregates of protein molecules as well as the particles. Scattering data for a sample of the *M. oleifera* protein in D_2O at a concentration of 2 mg ml^{-1} is shown as Figure S1 in the supporting information. The data in Fig. 2 were fitted using a model of core-shell particles that is implemented in the SASview software [50]. The fits were constrained to include a background from aggregates that was approximately proportional to the concentration of added protein and varied as about $Q^{-(2.5\pm0.1)}$. In principle separate terms for aggregates of both protein and particles could be included but as data for multiple isotopic contrasts are not available, it is not possible to make unambiguous fits for this component of the scattering. Small allowances for differences in contrast of the solvent assessed from about 1% variation in transmission were needed to optimize the fits.

A number of alternative models were tested against the data but the requirement to fit the small but noticeable second maximum in the sample with 5 mg ml^{-1} of added protein required a layer on the particles with increased adsorption. From the initial characterization, the radius, polydispersity and scattering length density of the particles were known. Fits of the thickness and scattering length density of the shell could therefore be used to determine the adsorbed amount. The volume fraction of protein was calculated from the scattering length density of the shell layer.

This was multiplied by the thickness and density to obtain the mass per unit area. Although the analysis provides reasonable information about the adsorbed amount, the thickness of the protein is only known within the broad range of about 10–30 Å as the shape and width of the peaks seen in the data in Fig. 2 are not well-defined.

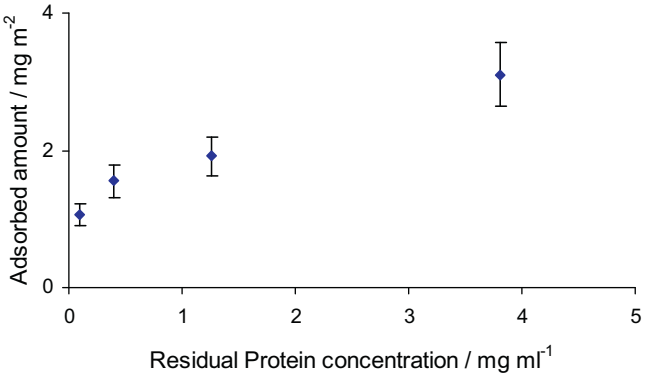

Fig. 3. Adsorption isotherm for *Moringa oleifera* protein on the deuterated latex PSD1 deduced from the fit parameters of the models shown with the data in Fig. 2. Excess is shown against the residual concentration of protein in solution.

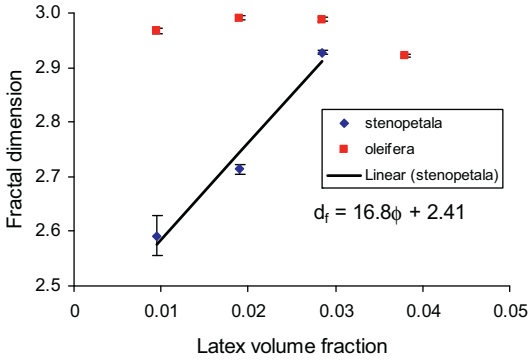

Fig. 5. Observed dependence on volume fraction of particles of the fractal dimension for samples with mass fraction 2 mg ml^{-1} *Moringa oleifera* (red squares) and 2 mg ml^{-1} *Moringa stenopetala protein* (blue diamonds). The scattering data and fitted model functions are shown in Fig. 4. (For interpretation of the references to color in this text, the reader is referred to the web version of the article.)

The layer thickness tended to increase with protein concentration. The adsorbed amount is shown in Fig. 3. Opposite charge of the cationic protein and anionic latex particles, indicated by the zeta potentials, provides an obvious mechanism for initial adsorption. The adsorption reaches about 3 mg m^{-2}. This is slightly less than that seen at hydrophilic surfaces such as silica [10] but may be understood as the polystyrene particles have a low surface potential with ionizable groups that are interspersed regions of more hydrophobic polystyrene. The thickness of the layer that is identified from the scattering is weighted by the density profile and this precludes detailed descriptions of the profile such as those obtained for absorption to silica in the studies that used neutron reflection [10]. The tendency for the observed thickness to increase with concentration would be consistent with multilayer adsorption as observed previously [10]. There is no direct data for adsorption of the *M. stenopetala* protein to polystyrene latex, however recent neutron reflection experiments (unpublished) have shown that it binds to both silica and alumina giving similar surface coverage and structure of bound layers as the *M. oleifera* protein.

Although aggregation can be seen from the upturn in intensity at low *Q*, and this indicates that the adsorbed protein was acting as a flocculent, the range of these measurements did not provide sufficient information to obtain details of the aggregate structure and so separate measurements were made using USANS.

4.2. USANS-scattering from flocculated particles

The two latex samples have similar surface potential and it was convenient to use the larger particles, PS3, for the USANS study. Preliminary tests showed that they underwent rapid flocculation and consequent sedimentation when solutions of *M. oleifera* protein were mixed by gentle shaking with the dispersion. Samples were prepared with different concentrations of latex, with mass fractions between 0.01 and 0.04, and 2 mg ml^{-1} of either *M. oleifera* or *M. stenopetala* protein. The dispersions and solutions were prepared in H_2O and the contrast of the large particles dominates the scattering for this system. In order to avoid problems of sedimentation, the sample cells were mounted on a rotating stage during the measurements. The USANS data are shown in Fig. 4.

The fits to the Teixeira model [24] of fractal aggregates are shown and the fractal dimensions that were obtained from the fits are plotted as a function of concentration in Fig. 5. It is apparent from the data and the values of *d* that the flocs are dense aggregates. For the *M. oleifera* protein, *d* is always close to 3 which corresponds to the maximum possible packing. This shows that the protein is very effective as a flocculent material. The values of the fractal dimension *d* for the *M. stenopetala* protein are less and show a systematic trend of an increase with particle concentration.

In USANS experiments there is often a concern about possible effects of multiple scattering on measurements as samples usually have rather large scattering cross-sections if the signal is to be measurable. These effects are most noticeable when there are sharp minima in scattering curves like those seen for dispersions of monodisperse spheres [51,52]. Abrupt changes in slope can also be perturbed by multiple scattering but the particular case of scattering from fractal has been addressed [53,54]. Provided a sufficient range of approximately linear data is available between the limits

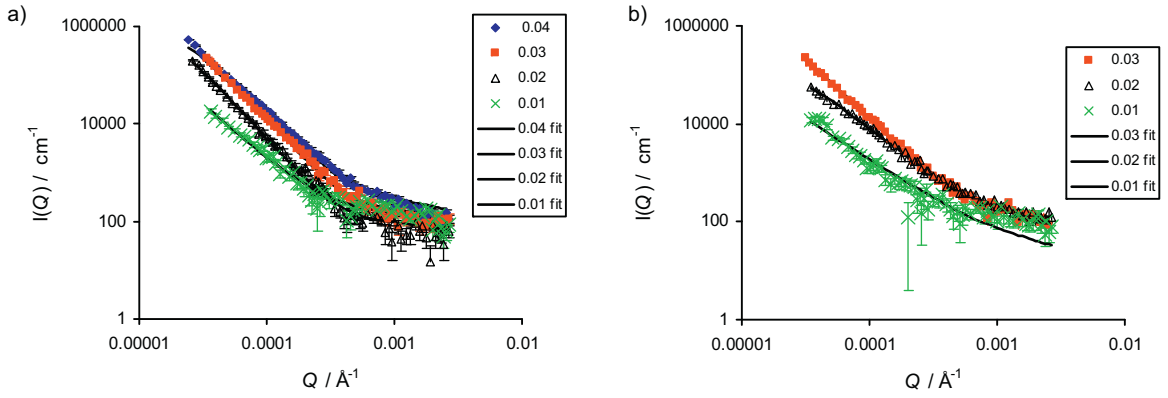

Fig. 4. Ultra small-angle scattering from flocculated hydrogenous latex, PS3, (a) with *Moringa oleifera*. Different particle concentrations (mass fraction) are shown with fits, (b) flocculated PS3 with *Moringa stenopetala* protein.

imposed by the overall aggregate size at small Q and the finite dimensions of the building blocks, in this case latex spheres, at high Q, the error in determining the fractal dimension is small. As the density of the aggregates is of primary interest, the discussion will centre on this quantity. The very large size of the flocs that show correlation sizes of more than 10 μm means that this quantity is not readily determined even from the USANS experiments.

In the case of *M. stenopetala* less dense flocs were observed when the protein was used at a concentration of 2 mg ml^{-1}. A markedly higher level of compaction of aggregates is seen with increasing particle concentration. An almost linear increase in the fractal dimension of the flocs can be seen in Fig. 5. In contrast there is very little change in the flocs with *M. oleifera* as the concentration of particles was changed since the clusters were already dense at the lowest concentration ($d > 2.9$). Simulations using Brownian dynamics predict [37] these high fractal dimensions for volume fractions of particles, φ that are of the order of 0.35 for DLCA. However charged colloids interact at long distance compared with their actual size and thus the effective volume fraction for dynamic processes can be much higher than that of the bare particles. The theoretical concepts of such effective increased radii have been described generally by Barker and Henderson [55] and the idea has been applied to rationalize the viscoelastic properties of polystyrene latex [56]. In this case the particle dimensions are approximately increased by the Debye screening length to give a larger interaction radius. In experiments with deionized water and with adsorbed protein it is not clear what would be the screening length but for an ionic strength of 4×10^{-5} mol l^{-1} the screening length is almost 50 nm and that might correspond to five-fold increase in volume fraction. If the trends for RLCA processes were similar to those for DLCA, higher values of d at a given concentration would be expected. The results therefore suggest that effects of concentration and hydrodynamic interactions may be important in determining final structures of flocs. A further study of these effects of both changing the concentration of added salt and directly altering the particle volume fraction on the aggregation would be interesting.

The aggregation and changes of floc structure with time were rapid. The USANS experiments allowed the lowest Q part of the scattering to be measured in about half an hour. Fig. 6 shows the results of repeating the measurements immediately after the initial mixing using *M. oleifera* protein as flocculent. A small change consistent with growth of the flocs is observed but it is difficult to make a full analysis of a small part of the curve. Some other samples with a particle volume fraction of 0.04 were the subject of repeat measurements after about 3 days and no further changes were seen. The effects of adding small amounts of salt (0.5 and 1×10^{-3} mol l^{-1} NaCl) were insignificant and the comparison of measurements in deionized water and in the presence of 0.5 and 1×10^{-3} mol l^{-1} NaCl is shown in Fig. 7. No significant difference is observed within the experimental uncertainties.

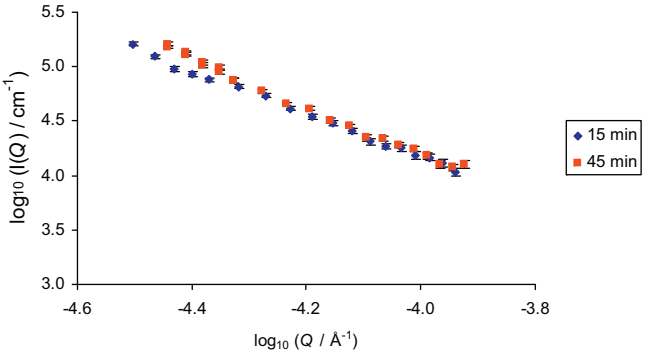

Fig. 6. Changes with time during early stages of flocculation for a sample with particle mass fraction 0.03 and 2 mg ml^{-1} *Moringa oleifera*.

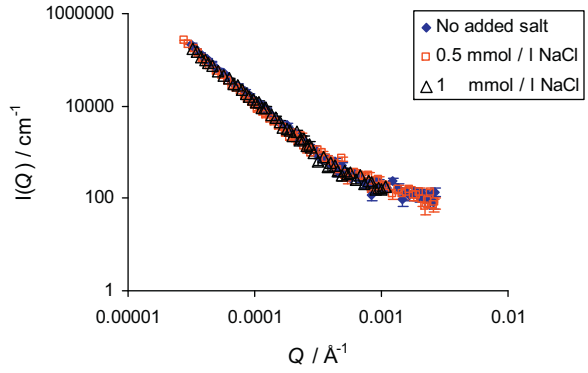

Fig. 7. Scattering for samples with particle mass fraction 0.03 and 2 mg ml^{-1} *Moringa oleifera* with added sodium chloride. No significant differences were observed when increasing the screening of charged interactions.

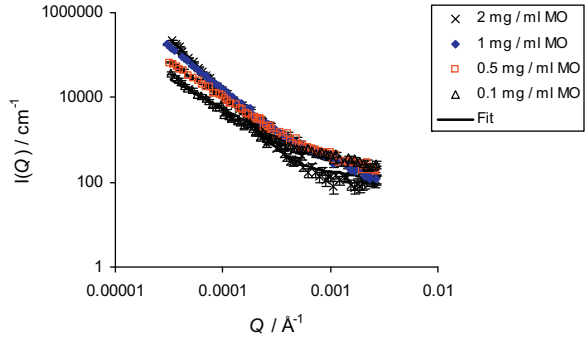

Fig. 8. The change in scattering from aggregates formed from latex with mass fraction 0.03 and different concentration of *Moringa oleifera* protein.

A series of experiments with different amounts of the *M. oleifera* protein and latex at a volume fraction of 0.03 were made and the scattering results are shown in Fig. 8. The scattered intensity at small Q and the slope of the log I versus Q curves increase with increasing concentration. Dispersions of latex with protein concentrations in the range 0.5–2 mg ml^{-1} were investigated. All other experiments were conducted with a concentration of 2 mg ml^{-1} as this was expected to provide saturated coverage of the particles with adsorbed protein. Even at substantially lower concentrations the flocculation is effective but the density of the flocs is less as seen in Fig. 9. This suggests that possibly partial coverage with protein causes adhesion of particles only at particular points on the surface and that this causes lower fractal dimensions. Alternatively free protein in solution may assist in the collapse of aggregates as it is

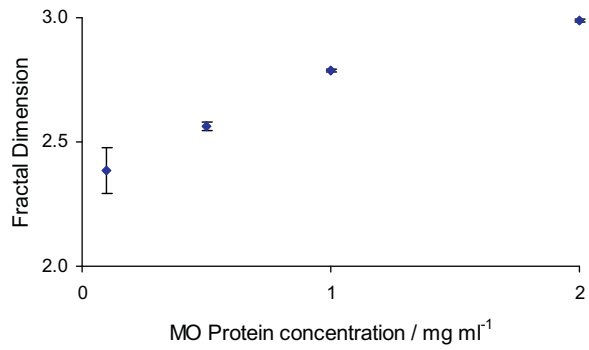

Fig. 9. Effect of changing *Moringa oleifera* protein concentration-fractal dimensions derived from the fits shown in Fig. 8.

likely to associate both with adsorbed protein and in solution. If the coverage at the surface were to saturate by about 4 mg m^{-2} then at all concentrations of large hydrogenous particles, there is sufficient protein to cover the surface. The slope at low momentum transfer seen in the double logarithmic plot of scattered intensity versus Q, about −2.5, for *M. oleifera* protein shown in Fig. 2 is lower than the fractal dimensions of particle aggregate formed with the protein that are reported in Fig. 5. This is attributed to the contribution of scattering from protein aggregates that may be less dense than particle aggregates. It should be noted that optimized use of proteins as a flocculent would select conditions with as little residual unadsorbed material as possible remaining in solution.

It is interesting to compare the fractal dimensions with those found using other flocculents. A review by Jefferson and Jarvis [57] has described flocs formed using materials such as aluminium sulfate, iron chloride and a synthetic cationic polymer. For natural organic matter these gave values of d_f of 2.2, 1.7 and 1.99 respectively. These fall in the range expected for DLCA and RLCA processes in dilute dispersions but are also lower than the values observed in the present study with *Moringa* proteins.

There are some important observations that arise from the data: the flocs formed by the low molecular mass proteins are quite different to those that are typically created with conventional flocculent polymers: high molecular mass and adsorption that bridges across particles often create large flocs that are of low density. The association of the particles is not just neutralization and subsequent reversal of charge. Under these circumstances restabilisation could occur when the charge is reversed. The tendency of the protein molecules to aggregate apparently dominates over charged repulsion. This tendency is also seen in the molecular aggregation that was observed in solutions of the protein on its own.

Unfortunately it is difficult to observe the particles and flocs directly when they are immersed in water as conventional microscopy techniques cannot be applied to the opaque samples. The scattering indicates that after some minutes the aggregate size is more than 10 μm and that if tumbling is stopped heterogeneous regions on the scale of one or a few millimetres could be observed before sedimentation occurred.

The analysis of amino acids for *M. stenopetala* protein provided as Table S2 should add to the knowledge of this material. There has been an interesting report concerning binding of heavy metal [58], however differences in efficacy of crude *M. stenopetala* and *oleifera* seeds, rather than extracted protein, as a flocculent may arise in part from the different yield of oil and protein [59] as well as the molecular composition and structure.

5. Conclusions

Our conclusions from these experimental studies fall in distinct areas that relate to fundamental aspects of flocculation of relevance to problems in water purification, specifically with seed protein as flocculent and to more general aspects of the colloid physics of aggregation. The initial measurements indicated that a layer of *M. oleifera* seed protein binds closely to the surface of polystyrene latex particles. This trend to adsorb to particles with some surface regions that are hydrophobic and other parts with charged groups such as sulfate moieties can assist in heteroflocculation. Proteins from two species of *Moringa* trees were investigated as flocculents and both gave rise to dense aggregates. The higher fractal dimension that corresponds to denser flocs was obtained with the extract from *M. oleifera* but also the *M. stenopetala* protein provides flocs that are more compact than those reported in studies with most ionic and polymeric flocculents. These structures are favourable for removal of impurities and for eventual dewatering of sludge.

The fractal dimensions observed are much larger than those reported for DLCA models and even, under most conditions, for RLCA processes. The rapid flocculation prevents detailed studies that would elucidate more details of the aggregation kinetics but the observation on products suggest that the protein may assist in rearrangement of particles until the most dense structures are obtained as expected when the limiting process is dominated by reaction rather than the diffusion of particles [17]. In this respect dynamic equilibrium of protein molecules in solution with adsorbed material at the particle interfaces and kinetics of protein rearrangement could be important as a means to further increase the density and fractal dimension of flocs. It is interesting to note that even with particles that are relatively large compared to those investigated in previous studies [17], the flocs are dense.

There have been some reports previously of changes in structure when flocs form in concentrated dispersions. This is of importance as the late stages of aggregation are always likely to involve higher local concentrations as cluster will float or sediment. The previous studies have mostly relied on simulations as investigation of the interior of concentrated colloidal dispersions is often difficult because the samples will be opaque and scatter light strongly. The observed increases in the fractal dimension with particle concentration for the samples with *M. stenopetala* protein resemble those predicted in simulations. However the fractal dimensions are higher and suggest that an increased effective volume fraction that might be attributed to long range particle interactions is needed to scale the computational model to the data.

This experimental study has also demonstrated the successful exploitation of the new tumbling [41] mounts for cells on the USANS instrument and thus shown that a wider range of samples can be investigated readily. This would allow more detailed studies of concentrated particles as the aggregate under a range of different conditions.

Acknowledgements

We are grateful to Anders Olsson who designed the rotating mounts used in the USANS measurements. Anna Källgren kindly obtained the *Moringa stenopetala* seeds in Ethiopia. Paul Butler is thanked for encouraging us to perform the USANS experiments. We acknowledge the support of the National Institute of Standards and Technology (NIST), U.S. Department of Commerce, in providing the neutron research facilities used in the experiments. This work utilized facilities supported in part by the National Science Foundation under Agreement no. DMR-0944772. The work in Sweden, Botswana and Namibia has been supported by the Swedish Research Council (VR/SIDA) Research Links grant with reference 348-2011-7241 and in part by the Office of Research and Development (ORD), University of Botswana.

Appendix A. Supplementary data

Supplementary data associated with this article can be found, in the online version, at http://dx.doi.org/10.1016/j.colsurfa.2013.11.038.

References

[1] M. von Smoluchowski, Z. Phys. Chem. 92 (1917) 129–168.
[2] B.B. Mandelbrot, Les Objets Fractals: Forme, Hasard et Dimension, Flammarion, Paris, 1975.
[3] D.W. Schaefer, J.E. Martin, P. Wiltzius, D.S. Cannell, Phys. Rev. Lett. 52 (1984) 2371–2374.
[4] P. Meakin, R. Jullien, J. Chem. Phys. 89 (1988) 246–250.
[5] American Water Works Association, Water Treatment, 4th edition, 2010.
[6] M.F. Chong, in: S.K.R. Sharma, R. Sanghi (Eds.), Advances in Water Treatment and Pollution Prevention, Springer Science + Business Media, Dordrecht, 2012, pp. 201–230.
[7] S.A. Muyibi, L.M. Evison, Water Res. 29 (1995) 2689–2695.

[8] A.F.S. Santos, P.M.G. Paiva, J.A.C. Teixeira, A.G. Brito, L.C.B.B. Coelho, R. Nogueira, Environ. Technol. 33 (2012) 69–75.
[9] A. Ndabigengesere, K.S. Narasiah, B.G. Talbot, Water Res. 29 (1995) 703–710.
[10] H.M. Kwaambwa, M. Hellsing, A.R. Rennie, Langmuir 26 (2010) 3902–3910.
[11] H.M. Kwaambwa, A.R. Rennie, Biopolymers 97 (2012) 209–218.
[12] F.K. Amagloh, A. Benang, Afr. J. Agric. Res. 4 (2009) 119–123.
[13] H.A. Jerri, K.J. Adolfsen, L.R. McCullough, D. Velegol, S.B. Velegol, Langmuir 28 (2012) 2262–2268.
[14] J. Beltrán-Heredia, J. Sánchez-Martín, A. Munoz-Serrano, J.A. Peres, Chem. Eng. J. 188 (2012) 40–46.
[15] I. Bodlund, Coagulant Protein from Plant Materials: Potential Water Treatment Agent, Licentiate Thesis, Biotechnology, KTH, Stockholm, 2013.
[16] P.W. Schmidt, J. Appl. Cryst. 24 (1991) 414–435.
[17] M.Y. Lin, H.M. Lindsay, D.A. Weitz, R.C. Ball, R. Klein, P. Meakin, Proc. R. Soc. Lond. A 423 (1989) 71–87.
[18] M.Y. Lin, H.M. Lindsay, D.A. Weitz, R.C. Ball, R. Klein, P. Meakin, Phys. Rev. A 41 (1990) 2005–2020.
[19] M.Y. Lin, R. Klein, H.M. Lindsay, D.A. Weitz, R.C. Ball, P. Meakin, J. Colloid Interface Sci. 137 (1990) 263–280.
[20] C.M. Sorensen, A. Chakrabarti, Soft Matter 7 (2011) 2284–2296.
[21] D.H. Bache, Chem. Eng. Sci. 59 (2004) 2521–2534.
[22] D.C. Mays, J. Environ. Eng. 136 (2010) 475–480.
[23] C.M. Sorensen, Aerosol Sci. Technol. 35 (2001) 648–687.
[24] J. Teixeira, J. Appl. Cryst. 21 (1988) 781–785.
[25] P. Sandkühler, M. Lattuada, H. Wu, J. Sefcik, M. Morbidelli, Adv. Colloid Interface Sci. 113 (2005) 65–83.
[26] M.L. Broide, R.J. Cohen, J. Colloid Interface Sci. 153 (1992) 493–508.
[27] J. Gregory, J. Colloid Interface Sci. 42 (1973) 448–456.
[28] G.K. von Schultess, B.G. Benedek, R.W. de Blois, Macromolecules 13 (1980) 939–945.
[29] (a) M. Carpineti, M. Giglio, Phys. Rev. Lett. 68 (1992) 3327–3330;
(b) M. Carpineti, M. Giglio, Phys. Rev. Lett. 71 (1993) 456 (Erratum).
[30] M. Carpineti, M.J. Giglio, Phys. Condens. Matter 6 (1994) A329–A332.
[31] M. Carpineti, M. Giglio, Phys. Rev. E 51 (1995) 590–596.
[32] F. Sciortino, P. Tartaglia, Phys. Rev. Lett. 74 (1995) 282–285.
[33] F. Sciortino, A. Belloni, P. Tartaglia, Phys. Rev. E 52 (1995) 4068–4079.
[34] H. Wu, M. Lattuada, M. Morbidelli, Adv. Colloid Interface Sci. 195–196 (2013) 41–49.
[35] K.W. Chau, Water Sci. Technol. 50 (2004) 119–124.
[36] R.M. Wu, D.J. Lee, T.D. Waite, J. Guan, J. Colloid Interface Sci. 252 (2002) 383–392.
[37] M. Lattuada, J. Phys. Chem. B 116 (2012) 120–129.
[38] A.E. González, F. Martínez-López, A. Moncho-Jordá, R. Hidalgo-Álvarez, J. Colloid Interface Sci. 246 (2002) 227–234.
[39] A.E. González, F. Martínez-López, A. Moncho-Jordá, R. Hidalgo-Álvarez, Phys. A Stat. Mech. Appl. 314 (2002) 235–245.
[40] J.G. Barker, C.J. Glinka, J.J. Moyer, M.H. Kim, A.R. Drews, M. Agamalian, J. Appl. Cryst. 38 (2005) 1004–1011.
[41] A. Olsson, M.S. Hellsing, A.R. Rennie, Meas. Sci. Technol. 24 (2013) 105901.
[42] S.R. Kline, J. Appl. Cryst. 39 (2006) 895–900.
[43] D22, http://www.ill.eu/instruments-support/instruments-groups/instruments/d22/
[44] M.A. Singh, S.A. Ghosh, R.F. Shannon, J. Appl. Cryst. 26 (1993) 787–794.
[45] J.W. Goodwin, J. Hearn, C.C. Ho, R.H. Ottewill, Colloid Polym. Sci. 252 (1974) 464–471.
[46] R. Maikokera, H.M. Kwaambwa, Colloids Surf. B Biointerfaces 55 (2007) 173–178.
[47] H.M. Kwaambwa, R. Maikokera, Colloids Surf. B Biointerfaces 60 (2007) 213–220.
[48] A. Ndabigengesere, K.S. Narasiah, Water Res. 32 (1998) 781–791.
[49] I. Berts, G. Fragneto, L. Porcar, M.S. Hellsing, A.R. Rennie, 2013 (submitted for publication).
[50] SASview 2.1 http://www.sasview.org/
[51] J.R.D. Copley, J. Appl. Cryst. 21 (1988) 639–644.
[52] A.R. Rennie, M.S. Hellsing, K. Wood, E.P. Gilbert, L. Porcar, R. Schweins, C.D. Dewhurst, P. Lindner, R.K. Heenan, S.E. Rogers, P.D. Butler, J.R. Krzywon, R.E. Ghosh, A.J. Jackson, M. Malfois, J. Appl. Cryst. 46 (2013) 1289–1297.
[53] Z. Chen, P. Sheng, D.A. Weitz, H.M. Lindsay, M.Y. Lin, P. Meakin, Phys. Rev. B 37 (1988) 5232–5235.
[54] M. Lattuada, H. Wu, M. Morbidelli, Phys. Rev. E 64 (2001) 061404.
[55] J.A. Barker, D. Henderson, Rev. Mod. Phys. 48 (1976) 587–671.
[56] R. Buscall, J.W. Goodwin, M.W. Hawkins, R.H. Ottewill, J. Chem. Soc. Faraday Trans. 78 (1982) 2889–2899.
[57] B. Jefferson, P. Jarvis, Practical application of fractal dimension, in: G. Newcombe, D. Dixon (Eds.), Interface Science in Drinking Water Treatment: Theory and Applications, Elsevier Ltd., Oxford, UK, 2006 (Chapter 4).
[58] L.M. Mataka, S.M.I. Sajidu, W.R.L. Masamba, J.F. Mwatseteza, Int. J. Water Resour. Environ. Eng. 2 (2010) 50–59.
[59] E. Seifu, J. Biol. Sci. 12 (2012) 197–201.